QUETZAL MINI, USB-C powered Sodium-Ion compatible battery charger performance evaluation

Andrei FOCA

National College ”Mircea cel Batrân” Constanța, Romania

focaandrei30@gmail.com

Abstract: Hobbyists and the RC industry have relied on Lithium batteries for years as their primary source of power, but with the emergence of a new technology, based on Sodium-Ion, there is now a greener alternative (Cai et al., 2024). Yet, few have replaced their batteries, and for good reasons, because most of the hobby chargers available today do not state to be supporting the new chemistry. This paper evaluates the results of several tests done on a custom theoretical maximum 66W battery charger and balancer, the QUETZAL MINI, using batteries ranging from 1 to 4 cells in series. The highest stable output recorded on a sodium-ion battery is approximately 62.4 W (16 V at 3.9 A), maintaining temperatures below 85°C.

Keywords: Na-Ion Compatibility, Battery Charger, USB-C PD 3.0, Active Balancing, 2S2P, 1S1P-4S1P, CC, CV, epoch.

QUETZAL MINI, evaluarea performanței unui încărcător de baterii alimentat prin USB-C, compatibil cu tehnologia de ioni de sodiu

Rezumat: Hobbyiștii și industria RC s-au bazat pe bateriile cu litiu de ani de zile ca sursă principală de energie, dar, odată cu apariția unei noi tehnologii, bazată pe ioni de sodiu, există acum o alternativă mai ecologică (Xiaosheng Cai et al., 2024). Cu toate acestea, puțini au înlocuit bateriile, și din motive întemeiate, deoarece majoritatea încărcătoarelor pentru modelele de hobby disponibile astăzi nu susțin noua tehnologie chimică. Această lucrare evaluează rezultatele mai multor teste efectuate pe un încărcător și echilibrator de baterie personalizat, cu putere teoretică maximă de 66 W, QUETZAL MINI, utilizând baterii între 1 și 4 celule conectate în serie. Puterea maximă stabilă înregistrată pe o baterie cu ioni de sodiu este de aproximativ 62,4 W (16 V la 3,9 A), menținând temperaturile sub 85°C.

Cuvinte cheie: compatibilitate Na-Ion, încărcător de baterii, USB-C PD 3.0, echilibrare activă, 2S2P, 1S1P-4S1P, CC, CV, epoch.

1. Introduction

Research on Sodium-Ion batteries began back in the 1990s, but it wasn’t until the 2010s and early 2020s that the technology started gaining traction in the scientific and hobbyist community (Zhao et al., 2023). As they became commercially available, a few Sodium-Ion cells were acquired in 2023 from Alibaba. To verify their authenticity, the cells were tested and confirmed to be genuine following a successful full discharge to 0V under safe conditions, which was a promising result.

Motivated by the potential of Sodium-Ion batteries, in April-May 2024, work began on a custom version of a charger for Na-Ion and Li-Ion cells that would be easy to use, completely Bluetooth configurable and equipped with active cooling, specifically designed for hobbyists who want to charge their small RC car/drone batteries, as the industry valuation is projected to increase (Mali, 2024). At the 4th generation of the PCB, which solved previous issues regarding parasitic elements and an unstable switching loop, on the 1st of November 2024, the QUETZAL MINI charged its first 2S1P 2600mAh battery pack. Figure 1 shows the top and bottom views of the assembled PCB.

https://doi.org/10.33436/v34i4y202403

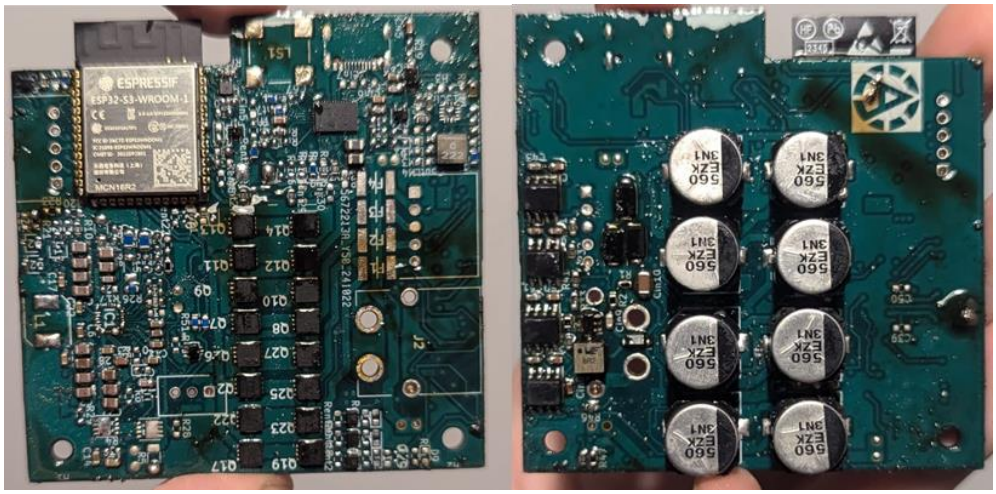

Figure 1. On the left, the top side of the PCB of the QUETZAL MINI, without the XT60/JST ports. On the right, the bottom side of the PCB (own research)

2. PCB architecture

The concept of the PCB involves separating the battery charging and balancing functions, by having 2 different functional blocks that are controlled by using an MCU, in our case an ESP32-S3 with an integrated antenna. In short, this configuration allows one to command the 2 blocks independently of each other. The architecture can be boiled down to the schematic below. Unidirectional arrows indicate the flow of power or data in the direction pointed by the arrow, while bidirectional arrows allow flow in both directions (see Figure 2).

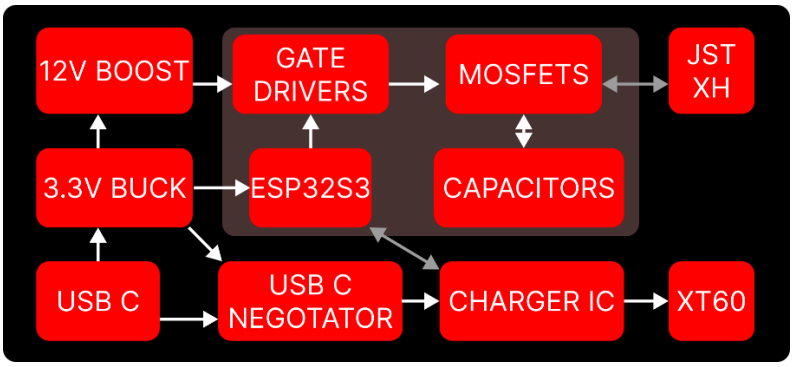

Figure 2. Simplified schematic of the QUETZAL MINI internal architecture with all sub-assemblies connected using arrows (own research)

2.1. Charging circuit

As the European Union voted for a standardised USB-C port for all mobile devices by 2024 (Fingas, 2022), this project is designed to meet their requirements. For the charging circuit, in line with the bottom sequence in the architecture, a USB-C negotiator IC is needed to establish a 20V/3A or 20V/5A contact with our phone/laptop charger. Then, an IC should convert the input voltage to the required termination voltage at the XT60 connector. Therefore, the TPS25730 was chosen as the PD 3.1 negotiator, and the BQ25798 as the 1-4S buck-boost battery charger.

The BQ25798 is a fully integrated, switch mode with adjustable frequency, and buck-boost charger for 1-4S batteries (Texas Instruments, 2020). It features an adjustable charging voltage, which makes it compatible with Na-Ion's typical maximum of 4V/cell (depending on the manufacturer, it can also reach 4.3V) (Mukai et al., 2017). Because it eliminates the need for external switching FETs, it allows for a smaller footprint solution. Although the chip also supports MPPT, however, it is not used in this project.

The TPS25730 is a highly integrated, maximum 100W (20V-5A), sink-only USB Type-C and PD controller certified for PD 3.1 (Texas Instruments, 2023). The device comes in 2 formats: the “D” version with an integrated sink load switch, while the “S” version requires an external sink path. For simplicity reasons, the “D” version was chosen for this project. However, for any future improvements, the “S” version may reduce the power dissipation.

2.2. Balancing circuit

While there are many variations of balancing circuits, the QUETZAL MINI implements a series of N CHANNEL MOSFETs that work in 2 stages by connecting the aluminium organic polymer capacitors in parallel with each other or with the batteries (Pittaway, 2023). Each goes first through a 2A PPTC and then meets the first line of MOSFETs.

In-between the first and second line there are 2 560uF, 25VDC, 4000 Hour Life capacitors, amounting to a total of 1120 uF per cell. MOSFETs are controlled by 4 Half-Bridge gate drivers with an integrated bootstrap diode, each controlling two pairs of high and low-side MOSFETs (Green & Zheng, 2022).

During the first stage, the capacitors are tied to each of their corresponding battery cells. Depending on the voltage difference between the capacitor and the battery, the capacitors either charge or discharge. During the second stage, capacitors are brought in parallel with each other. In doing so, they are equalized to the same voltage.

2.3. Logic circuit, PCB stackup and assembly method

From the user interactions via Bluetooth to the I2C writes to the BQ25798 and balancing drivers control, an ESP32S3 MCU handles all operations. The chip is programmed via a JST 5-pin connector on the side of the PCB. The pin configuration is as follows:

- 8 I/Os for Half-Bridge gate drivers;
- 2 I/Os for I2C with the BQ25798;
- 2 I/Os for the TX/RX communication with the ESP32-S3 programmer;
- 2 EN/IO0 for the ESP32-S3 programming;
- 1 I/O for fan control;
- 1 I/O for buzzer control;
- 1 I/O for a debug led.

As per the recommended stackup for 6-layer PCBs, the project follows the classic SIGNAL/POWER, GND, POWER, SIGNAL, GND, SIGNAL/POWER path to ensure signal and power integrity (Peterson, 2022). The surface finish is made using ENIG 2U’’ and the material is FR-4 TG155. The procedure for mounting all parts on the PCB was conducted manually, assembling the heavier capacitors and parts on the bottom of the PCB using a hot plate. In contrast, the parts on the top of the PCB were soldered using hot air.

3. Programming

This paper will not dive into the details of the programming methods, however, there are 2 main components to discuss: the ESP32-S3 code and the application code. The ESP32-S3 code was, for the most part, developed in Arduino IDE, whereas the Bluetooth “QUETZAL” app was entirely programmed in Visual Studio Code using Flutter, a cross-platform mobile framework which allows app iterations to be made quickly and facilitates Bluetooth integration through its various libraries (Flutter Blue Plus, 2024). Currently, the application is only available on Android.

For uploading the code on the ESP32-S3, a self-designed PCB centred around the CP2102N USB-to-UART chip was used.

4. Equipment used and thermals

Five main measurement devices are required: one to read the battery voltages every 15 minutes (or epoch), one to read the current going in or out of the battery, one to visualise the USB PD contract, one to discharge batteries in the case of repeated tests, and one to establish the connection between the BQ25798 IC and the TI browser GUI for chargers.

As for the equipment, starting with the multimeter, a MAXWELL model MX25201 was used for reading battery cell voltages. For the current clamp, a PROSTER CM6000 Pro was used for reading the battery charge/discharge current. For the USB Tester, an FNB58 was used to visualize the USB PD contract, along with the power going into the device. For the electronic load tester, a DL24P was used to discharge batteries in between tests. Last but not least, a USB2ANY device from Texas Instruments is required to access the TICHARGER_GUI. The device connects to the I2C pins of the BQ25798 and makes communication possible.

The QUETZAL MINI was tested across different battery chemistries, cells count and capacities, with the results showing a maximum stable constant current charge of 3,8A, regardless of charging voltage, which doesn't matter in calculating dissipated power:

$$P = I^2 R \tag{1}$$

With the Rds(on) resistance for the integrated switching FETs being 24 & 35 mΩ on the buck side and 28 & 17mΩ for the low boost, the power dissipated, in this case, would come from the buck side, since the 20V PD contract is primarily used as an input, and that would be given by the equation:

$$3.8^2\,\mathrm{A} \times 0.024\Omega + 3.8^2\,\mathrm{A} \times 0.035\Omega \simeq 0.9W \tag{2}$$

With a 1 by 1cm aluminium heatsink on top, a 5.15W/mK thermal paste layer in between and a 60 X 60 X 10 fan mounted as an intake, the chip stays below 85C while charging at 3.8A on the output, under normal room temperature conditions. These measures, combined with an almost optimal layout of inner layers and surrounding complementary parts, provide satisfactory thermal management results for optimal functioning (Beck, 2023).

5. Results

The device was tested in 6 different scenarios, with all Na-Ion batteries completely depleted, having been discharged to about 10% power and then held in a short circuit for at least 15 minutes before the charging started, whereas the LiPO started at around 20% state of charge. For the Sodium Ion, 1/2/3/4S1P batteries were tested, all at 2600mAh capacity, and one 2S2P. In the case of the LiPO, it was a 3S1P, 2200mAh.

All measurements taken fall within the range of a 5% human error.

Across the charts, a "Mode" line will be graphed. It refers to the charging mode of the BQ25798. 0 is Trickle Charge (Fixed 100mA CC), 1 is Pre-Charge (Configurable, CC), 2 is Fast Charge CC (Configurable, CC mode only), 3 is Fast Charge Combined (for periods with both CC and CV) and 4 is Fast Charge CV (CV mode only).

For time reasons, all measurements were done in Fast Charge only, with Pre-Charge not being required. All tests except for the 1S1P Sodium-Ion, which was charged at 2.6A, were done at 3.8A CC. Voltage/current values were read using the multimeter/current clamp and the TI GUI.

5.1. Single-cell charge

The blue line represents the cell voltage, while the white line is the Mode. Because the beginning voltage of the single cell was below the 2.25 threshold, the BQ25798 applied a slow "Trickle Charge" of constant 100mA, which explains the difference between the first 2 timestamps

in Figure 3, coloured in red. The battery voltage increased a mere 0.48V in the first 134 minutes, while afterwards the 2.6A CC mode could be activated.

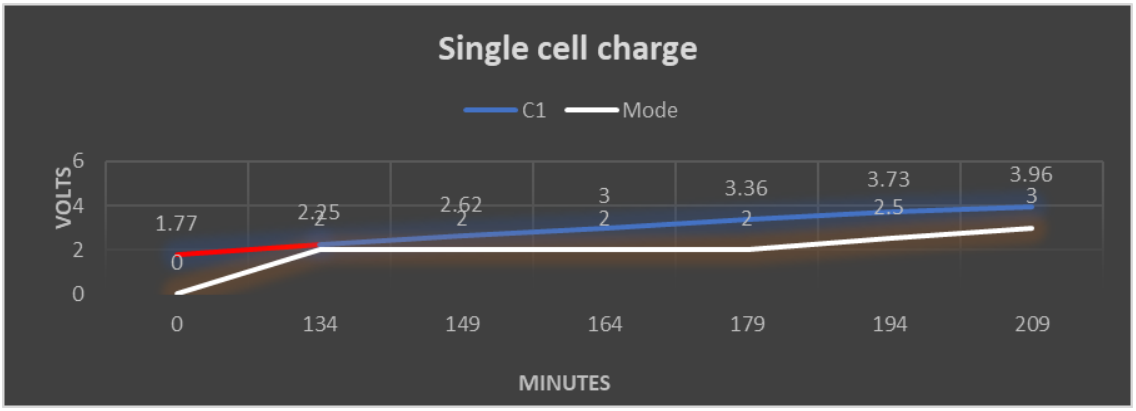

Figure 3. The charging chart for a single 1S1P 2600mAh Sodium-Ion battery at 3.8ACC, with an initial 0.1A Trickle Charge; the voltage is on the y-axis, minutes on the x-axis. (own research)

Single-cell batteries were observed to only allow a maximum of 2,6A of current, unlike their multi-cell counterpart. Na-Ion usually enters CV at around 3.6V/cell, which is where the 1C constant current charge stops.

5.2. Multi-cell standalone charge and temperature performance

In this section, solely the charge function of the BQ25798 will be evaluated, along with its temperature performance in various states of charging. Measurements were taken manually using the equipment previously mentioned.

After every 15 or 30 minutes, the battery was disconnected from the charger and the values were read because the current version of the QUETZAL MINI doesn't feature an independent cell voltage reading capability.

Blue columns are for the 2S, whites are for the 3S, and reds are for the 4S. All batteries started with their cells mostly in balance, with a +/-0.04V max difference.

Most cells started at roughly 1.7V and the voltage difference between each cell stayed the same until the end of the charge, with +/- 0.04V from the average, which is visible in Figure 4. The balancing circuit was disabled.

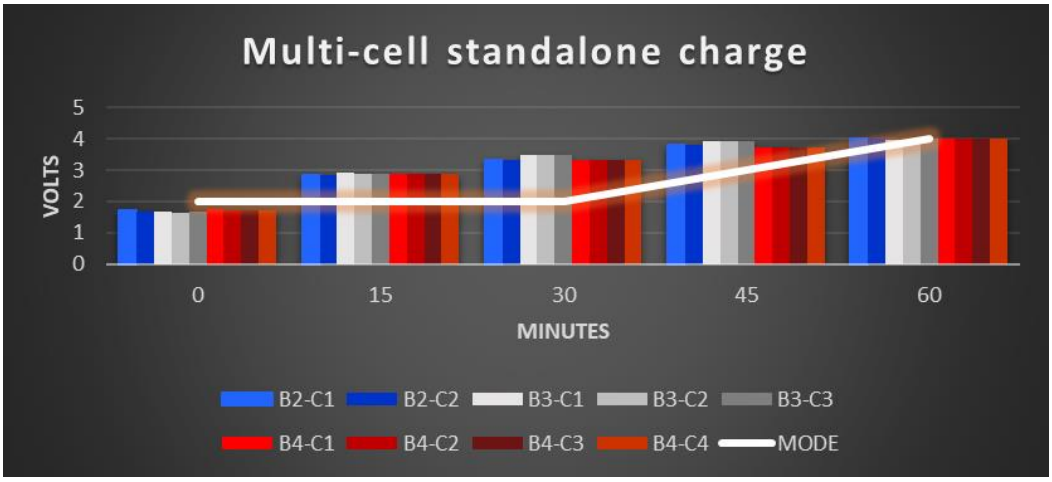

Figure 4. The charging chart for 2S/3S/4S1P 2600mAh batteries at 3.8A CC; the voltage is on the y-axis, and minutes on the x-axis. (own research)

As with the sodium cells, the 2200mAh 3S1P LiPO charge began with its cells within a +/- 0.04 V range of each other. It is important to note that the LiPO began from about 20% state of

charge as it could not be completely drained without dealing permanent damage, which is shown in Figure 5.

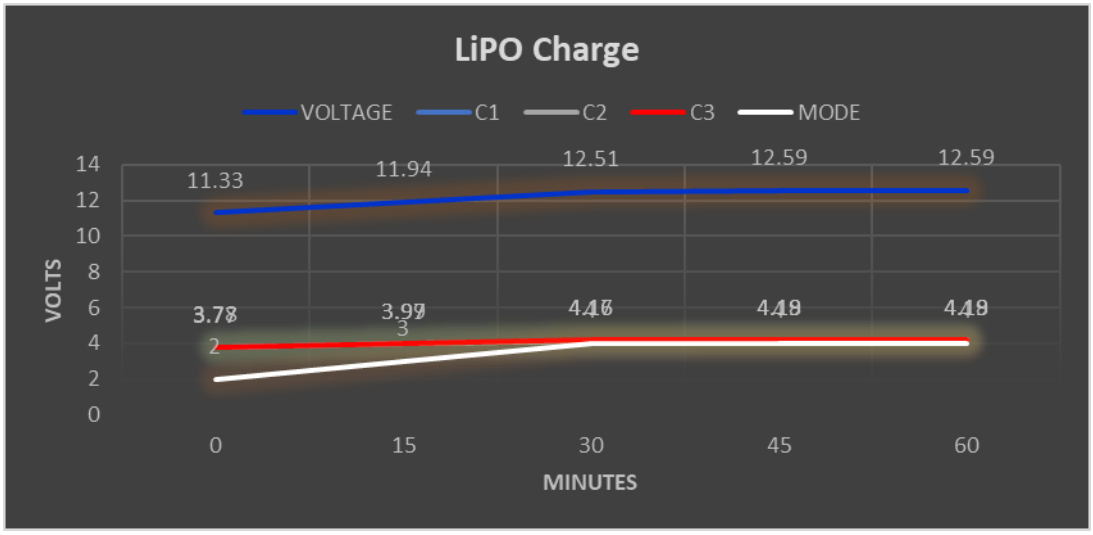

Figure 5. The charging chart for a 3S1P 2200mAh LiPO battery at 3.8A CC, the voltage on the y-axis, and minutes on the x-axis. (own research)

At a 1C charge, it demonstrated a smaller power hunger. Even though the charge current was set to 3,8A, the CC mode didn't last long and the chip changed to CV in the first 30 minutes of the charge.

The IC temperature reached its peak during the 3.8A CC charge and dropped the moment we transitioned into CV mode. Values were extracted from the IC ADC, using the TI charger GUI.

The temperature during CC mode was constant, while the transition to the CV mode also initiated the downturn of the temperature. As the current dropped below 1A, the chip approached near-room temperature, which can be observed in Figure 6.

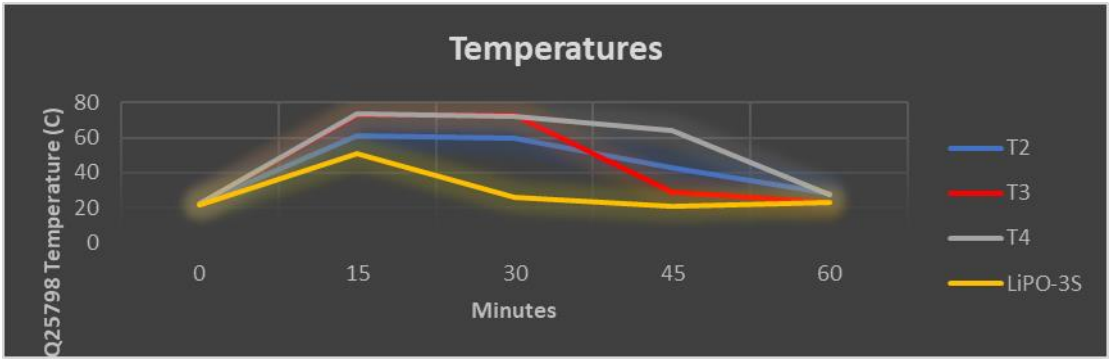

Figure 6. The BQ25798 ADC-read chip temperature during charging (1/2/3/4S1P Na-Ion, 3.8A CC charge); the read temperature is on the y-axis, minutes on the x-axis. (own research)

6. Balancing

As already mentioned, the QUETZAL MINI also supports active capacitive balancing for 2-4S packs. The balancing values were taken after a full charge of a 4S Sodium-Ion battery, and afterwards connecting it to the balancing port for 1 hour, at a switching frequency of 5kHz. Each cell was within +/- 0.03 after 1 hour, compared to +/-0.04 initially.

The performance is evaluated for 3 hours. Cells 1,2 & 3 stay constantly within a range of +/- 0.01V of their average, the 4th cell keeps being the most distant from the others, as seen in Figure 7.

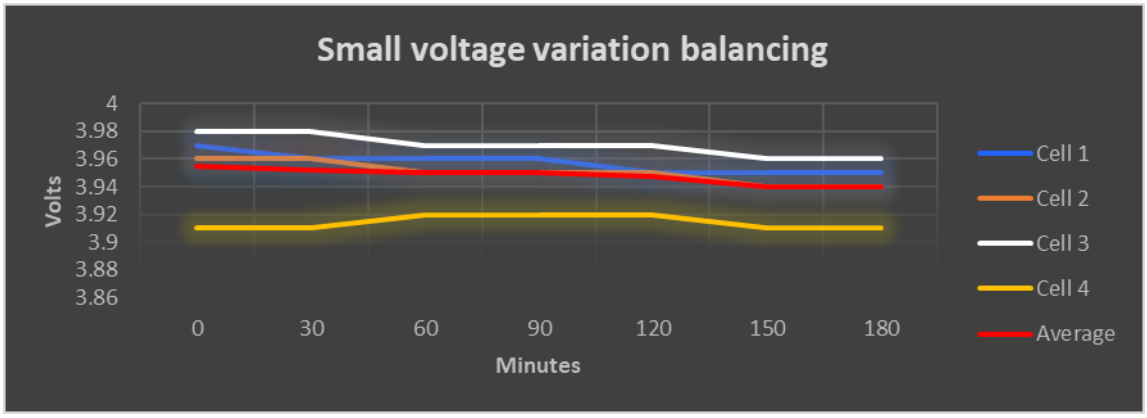

Figure 7. The equalization chart shows the voltages of each of the cells of a 4S1P 2600mAh Na-Ion during a 3-hour active balancing session; the voltage is on the y-axis, minutes on the x-axis. (own research)

The 4S pack from the first test was already balanced for the most part. However, it was also tested what difference the balancer would make to a battery with a much larger voltage discrepancy between its cells.

The second cell of a completely depleted Na-Ion battery pack was charged to 3.03, while the first cell was at only 1,72V. Data was gathered every 30 minutes for 3 hours, after which the battery was left to be balanced overnight. In the morning, both cells were equalised, with 2.72V each, as seen in Figure 8.

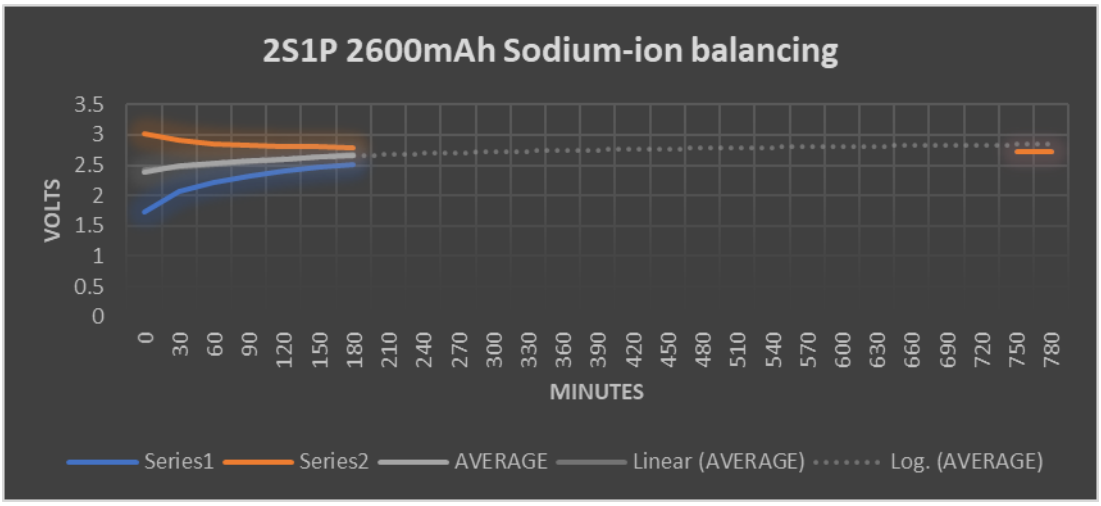

Figure 8. The equalization chart shows the voltage of each cell of a 2S1P 2600mAh Na-Ion during a 3-hour active balancing session and, after being left to balance overnight, in the morning; the voltage is on the y-axis, minutes on the x-axis. (own research)

7. Discussions

While the QUETZAL MINI has its limitations, possibly because of insufficient thermal management, possible lack of functionality for the 4th cell balancing driver or imperfect PCB routing, it can offer a small-factor solution to basic, everyday hobbyist needs. As this article is based around the 4th version of the PCB, there are still factors that can or must be improved, looking specifically at the balancing part which features a relatively small balancing current probably because of the high Rds(on) of 6.2mO relative to the alternatives available on the market that have at least 5 times less the current value, some even in the range of micro ohms. The relatively low switching frequency of 5 kHz was chosen to prevent conduction overlap between the high-side and low-side MOSFETs, which became problematic at frequencies above 10 kHz. However, it is important to note that the current circuitry is the first almost fully functional one produced, so as long as there is time, there is also room for improvement.

Whereas for charging, the results offered by the TI chip are satisfactory, as 3.8A at 16V, totalling 62.4W, is more than 94% of the 66W advertised sink capability of the charging chip. Attempting to go too much above 3.8A would result in distorted audible switching noise from the converter, along with current & voltage drops, signalling excessive parasitic elements, improper component placement or perhaps an insufficient ground plane coverage around the loop (Bhat & Nagaraja, 2014). Given the high component density around the chip and the various other copper traces from nearby sub-assemblies, along with the use of through vias instead of buried ones, the ground planes on the top and bottom sides were severely punctured unlike the 5th and 2nd layer of exclusive ground that should separate the high-frequency traces from the power ones. Perhaps the root of the problem is not particularly the physical placement of parts, but the choice of converter frequency. Indeed, a step-down from 1.5MHz to 750kHz may require a parts revision, but with a smaller frequency, the switching losses would be lower as well, at the cost of only a few more square centimetres in the PCB area (Xie & Guo, 2024).

Ultimately, the problem resumes to 3 factors: the solution size, thermal performance and layout effectiveness, both of the latter of which could be optimized by opting for a chip with an external switching loop if space is not a constraint as it was for this project.

In addition, if the QUETZAL MINI were compared with an available charging solution product, from the beginning, the QUETZAL MINI was designed to be a successor to the well-known and widely used hobby community battery charger, the S65 (SkyRC Technology Co. Ltd, 2022). Below, Figure 9 shows a direct comparison of the main attributes of each charger.

	Size (cm)	Compatible Chemistries	MAX Charging power (W)	Balancing Method	Can only balance?	Can discharge?	Cooling	Control method
QUETZAL MINI	7.6 x 7.6 x 4.9	Lithium/Sodium	62,4	Active	Yes	No	Active + Passive	Bluetooth
S65	11.8 x 11.5 x 4.5	Lithium, NiMH/NiCd	65	Passive	No	Yes	Active + Passive	Buttons

Figure 9. The chart highlights the differences between the QUETZAL MINI (2nd Row) and S65 (3rd Row) battery chargers. (own research)

The comparison chapters are: “Size” (cm), “Compatible (Battery) Chemistry”, “MAX Charging Power (W)”, “Balancing Method” (Active/Passive), “Can only balance” (if it has independent balancing), “Can discharge (the battery)” (Yes/No), “Cooling (Method)”, “Control method”. In the image above, boxes with a green background symbolise the better characteristic out of the 2 from the battery chargers, while red means the opposite, and orange means equal or that the superior can’t be determined.

Size-wise, the QUETZAL MINI is more compact, with the case measuring 7.6 x 7.6 x 4.9 cm (L X l X H), while the S65 measures 118 x 115 x 45mm.

In terms of compatible battery chemistries, unlike the S65 which only supports Lithium and NiMH/NiCd batteries, the QUETZAL MINI also supports the new Sodium-Ion batteries.

For the balancing power, the QUETZAL MINI and S65 charger are rated for approximately the same maximum of 65W. However, the QUETZAL MINI has only shown stable results up to 62.4W.

One important thing to note is the balancing method. Although it may not function properly for 4S batteries, the QUETZAL MINI has an active balancing method, which, unlike the passive method, allows for the balancing of the cells independent of charging.

One key feature present in the S65 is the ability to discharge batteries, which was not implemented in the design under discussion.

As for the cooling method, both chargers use a passive heatsink on top of the heating components along with a fan to regulate the temperature. In terms of user interface, the 2 feature a completely different approach, where the QUETZAL relies on a Bluetooth app and the S65 has an LCD screen with buttons. Both of these characteristics were grouped within the same paragraph and with the same colour since the cooling methods are the same, while the control methods cannot possibly be objectively compared since they both target specific user preferences.

REFERENCES

Beck, M. (2020) Thermal design concerns for buck converters in high-power automotive applications. *Analog Design Journal*. 2Q, 1-8. https://www.ti.com/lit/an/slyt793a/slyt793a.pdf?ts=1731735386728.

Bhat, S. & Nagaraja, H. N. (2014) Effect of Parasitic Elements on the Performance of Buck-Boost Converter for PV Systems. *International Journal of Electrical and Computer Engineering*. 4(6), 831-836. doi:10.11591/ijece.v4i6.6855.

Fingas, J. (2022) *The EU will require USB-C charging for mobile devices by the end of 2024*. Engadget, https://www.engadget.com/eu-usb-c-port-charging-requirement-approved-141546579.html [Accesse: 3rd of March 2024].

Flutter Blue Plus (2024) *Flutter plugin for connecting and communicating with Bluetooth Low Energy devices, on Android, iOS, and MacOS.* https://pub.dev/packages/flutter_blue_plus [Accessed: 28th May 2024].

Green, P.B. & Zheng, L. (2022) *Gate drive for power MOSFETs in switching applications. A guide to device characteristics and gate drive techniques*. Infineon Technologies AG, Munich, Germany. https://www.infineon.com/dgdl/Infineon-Gate_drive_for_power_MOSFETs_in_switchtin_applications-ApplicationNotes-v01_00-EN.pdf?fileId=8ac78c8c80027ecd0180467c871b3622 [Accessed: 29th May 2024].

Mali, S. (2024) *Remote Control Toy Car Market Report 2024 (Global Edition).* Cognitive Market Research. https://www.cognitivemarketresearch.com/remote-control-toy-car-market-report [Accessed 15th November 2024].

Mukai, K., Inoue, T. I., Kato, Y. & Shirai, S. (2017) Superior Low-Temperature Power and Cycle Performances of Na-Ion Battery over Li-Ion Battery. *ACS Omega*. 2 (3), 864-872. doi:10.1021/acsomega.6b00551.

Peterson, Z. (2022) *6-Layer PCB Stackup Design Guidelines.* Altium. https://resources.altium.com/p/6-layer-pcb-design-guidelines-pcb-design [Accessed 12th February 2024].

Pittaway, S. (2023) *How Does an Active Balancer Work?* Youtube. https://youtu.be/VR-G-3D82e0?si=Q8Linlg64y6vk5eN [Accessed: 2nd of May 2024].

SkyRC Technology Co., Ltd (2022) S65 AC Balance Charger/Discharger. *S65 Instruction Manual* V2.10. https://www.skyrc.com/s65 [Accessed 9th of May 2024].

Texas Instruments, Battery charger ICs (2020) *BQ25798 I2C Controlled, 1- to 4-Cell, 5-A Buck-Boost Battery Charger with Dual-Input Selector, MPPT for Solar Panels and Fast Backup Mode*, https://www.ti.com/product/BQ25798?keyMatch=BQ25798RQMR&tisearch=universal_search&usecase=OPN [Accessed 21st of May 2024].

Texas Instruments, USB Type-C & USB Power Delivery ICs (2023) *TPS25730 USB Type-C® and USB PD Controller with Integrated Power Switches Optimized for Power Applications.* https://www.ti.com/product/TPS25730?keyMatch=TPS25730&tisearch=universal_search&usecase=GPN-ALT [Accessed 21st of May 2024].

Xiaosheng Cai, X., Yingying Yue, Zheng Yi, Junfei Liu, Yangping Sheng, Yuhao Lu (2024) Challenges and industrial perspectives on the development of sodium-ion batteries. *Nano Energy*. 129, Part B, 110052. doi:10.1016/j.nanoen.2024.110052

Xie, H. & Guo, E. (2024) *How the Switching Frequency Affects the Performance of Buck Converter*. Texas Instruments. 1-10. https://www.ti.com/lit/an/slvaed3a/slvaed3a.pdf?ts=1731755946315 [Accessed 29th of April 2024].

Zhao, L., Zhang, T., Li, W., Li, T., Zhang, L., Zhang, X. & Wang, Z. (2023) Engineering of Sodium-Ion Batteries: Opportunities and Challenges, Engineering. *Engineering*. 24, 172-183. doi:10.1016/j.eng.2021.08.032.

Andrei FOCA is a 12th-grade student at "Mircea cel Bătrân" National College in Constanța, with a passion for electronics and robotics. Throughout his work, he has won four awards at international competitions in the field, including the "Award for Excellence in Technological Innovation" granted by the Dan Voiculescu Foundation in November 2024. His journey in the field began in October 2022 with a robotics kit designed for play, and since then, he has managed to create custom devices, ranging from simple sensors for smart home automation systems to a semi-humanoid robot prototype taller than himself. Andrei FOCA has acquired the necessary knowledge from independent sources, purchasing specialized books and delving into the information available online, demonstrating remarkable self-learning capabilities and technological innovation.

Andrei FOCA este elev în clasa a XII-a la Colegiul Național „Mircea cel Bătrân” Constanța, având o pasiune pentru electronică și robotică. În decursul activității sale, a obținut patru premii la concursuri internaționale de profil, printre care și „Premiul pentru Excelență în Inovație Tehnologică” acordat de către Fundația Dan Voiculescu în noiembrie 2024. Călătoria sa în domeniu a început în octombrie 2022, cu un kit de robotică destinat jocului, iar de atunci a reușit să creeze dispozitive personalizate, variind de la senzori simpli pentru sisteme de automatizare a locuințelor inteligente, până la un prototip de robot semi-uman mai înalt decât el. Andrei Foca și-a însușit cunoștințele necesare din surse independente, achiziționând cărți de specialitate și aprofundând informațiile disponibile pe Internet, demonstrând o capacitate remarcabilă de autoformare și inovație tehnologică.